

Copyright Notice

©2005 IEEE. Personal use of this material is permitted. However, permission to reprint/republish this material for advertising or promotional purposes or for creating new collective works for resale or redistribution to servers or lists, or to reuse any copyrighted component of this work in other works must be obtained from the IEEE.

(Article begins on next page)

An Electro-Thermal HBV Model

Mattias Ingvarson*, Josip Vukusic†, Arne Øistein Olsen*, T. Arezoo Emadi*, and Jan Stake*

*Microwave Electronics Laboratory, Department of Microtechnology and Nanoscience,
Chalmers University of Technology, SE-412 96 Göteborg, Sweden
Email: jan.stake@mc2.chalmers.se

†Institut d'Electronique et de Microélectronique du Nord,
UMR CNRS, Université des Sciences et Technologies de Lille,
59652 Villeneuve d'Ascq Cedex, France

Abstract—We present an electro-thermal model for heterostructure barrier varactors (HBVs). The model updates the device temperature and temperature-dependent device parameters self-consistently. Harmonic balance simulations with the model are presented, and the agreement with measured HBV tripler results is excellent. A design example of a 141-GHz high-power HBV tripler further demonstrates the use of the model.

Index Terms—Heterostructure barrier varactor, frequency multiplier, self-heating, high-power applications.

I. INTRODUCTION

High-power millimeter wave sources are needed for many new applications including e. g. medical and biological imaging systems and security systems [1]. A promising approach to the realization of such sources is to use frequency multipliers with heterostructure barrier varactors (HBVs) [2]. A major advantage of using HBVs rather than e. g. reverse-biased Schottky varactors is that the power handling capacity can be improved by stacking several barriers epitaxially, and thereby increasing the breakdown voltage. State-of-the-art output power level results from HBV frequency triplers of 1250 mW at 99 GHz [3], 10 mW at 210 GHz [4] and 9 mW at 247.5 GHz [5] have been demonstrated. However, the device geometries and circuit topologies used are generally optimized for a high conversion efficiency at high frequencies rather than for a maximum power handling capacity. Recently, a multi-mesa HBV geometry, designed to be able to handle power levels of several Watts around 100 GHz, has been suggested by the authors [6]. With conversion efficiencies in the best case around 20%, most of the pump power is dissipated in the device, causing very high peak temperatures in the active layers. High temperatures can cause material degradation leading to device failure, and also impair the multiplier performance even for low power levels [7], [8]. Therefore, thermal considerations are important for the design of layer structures and device geometries for HBVs. Simple analytical expressions can be used for initial estimations and investigations about thermal properties [9], but in order to properly design and analyze HBVs, especially for high-power applications, it is necessary to

employ combined electrical and thermal simulations. We present an electro-thermal HBV model, implemented in Agilent Advanced Design System (ADS).

II. ELECTRO-THERMAL MODEL

The voltage V_j across an HBV as a function of the charge Q stored in the device is calculated from the quasi-empirical Chalmers HBV model [10]:

$$V(Q) = N \left(\frac{bQ}{\varepsilon_b A} + 2 \frac{sQ}{\varepsilon_d A} + \text{Sign}(Q) \cdot \left(\frac{Q^2}{2qN_d \varepsilon_d A^2} + \frac{4k_B T}{q} \left(1 - \exp \left[-\frac{|Q|}{2L_D A q N_d} \right] \right) \right) \right) \quad (1)$$

where N is the number of barriers, b , ε_b , s and ε_d are the thickness and the permittivity of the barrier and spacer layers, respectively, A is the device area, q is the elementary charge, N_d is the doping concentration in the modulation layers, k_B is the Boltzmann constant, T is the device temperature, and L_D is the extrinsic Debye length,

$$L_D = \sqrt{\frac{\varepsilon_d k_B T}{q^2 N_d}}. \quad (2)$$

The displacement current is

$$i(t) = \frac{\partial Q}{\partial t}. \quad (3)$$

The conduction current is important in GaAs-based HBVs, but also present in InP-based devices, and can be described by empirical expressions,

$$I_{\text{cond, GaAs}} = a_{\text{GaAs}} \cdot A \cdot T^2 \sinh \left(\frac{E_b}{E_0} \right) \exp \left(-\frac{\phi_b}{kT} \right) \quad (4)$$

where E_b is the electric field in the barrier and a_{GaAs} , E_0 and ϕ_b are material constants [10], and

$$I_{\text{cond, InP}} = a_{\text{InP}} \cdot A \cdot \exp \left(\frac{T}{T_0} \right) \sinh \left(\frac{V}{V_0} \right) \quad (5)$$

where a_{InP} , T_0 and V_0 are material constants [11]. A temperature-dependent expression for the series resistance,

$R_s(T)$, is also needed. The series resistance depends on the device geometry, material parameters and temperature, and can, for planar HBVs, be estimated as

$$R_s(T) = R_c + R_{\text{active}}(T) + R_{\text{contact}}(T) + R_{\text{spread}}(T) \quad (6)$$

where R_c is the ohmic contact resistance, R_{active} is the resistance of the active layers, R_{contact} is the resistance of the contact layers, and R_{spread} is the spreading resistance in the buffer layer. Any of these resistances can be calculated as

$$R = \frac{t}{A \cdot \sigma} \quad (7)$$

where t is the thickness, A is the cross-sectional area and σ is the electrical conductivity of the layer. The electrical conductivity depends on the doping concentration and the electron mobility as

$$\sigma = q \cdot N_d \cdot \mu_e(N_d, T) \quad (8)$$

where $\mu_e(N_d, T)$ is the electron low-field mobility, calculated from the following empirical model [12]

$$\mu_e(N_d, T) = \mu_{\min} + \frac{\mu_{\max}(T_0)(T_0/T)^{\theta_1} - \mu_{\min}}{1 + \left(\frac{N_d}{N_{\text{ref}}(T_0)}(T/T_0)^{\theta_2} \right)^\lambda} \quad (9)$$

Here, μ_{\min} , μ_{\max} , N_{ref} , λ , θ_1 and θ_2 are fitting parameters available for most common III-V materials, and $T_0 = 300$ K. The thermal resistance R_{th} can be calculated analytically for simple geometries, but for typical HBV device geometries, full 3-D FEM simulations have to be employed [9]. The thermal capacitance C_{th} models the thermal storage of the device, so that the thermal time constant is $\tau_{\text{th}} = R_{\text{th}} \cdot C_{\text{th}}$. By using an equivalent electro-thermal circuit, the device temperature T can be treated like any other control voltage [13]. Now, the electrical properties of an HBV can be modeled with harmonic balance simulations using the equivalent circuit in Figure 1 (left) together with (1), combined with appropriate expressions for the conduction current and the series resistance. The thermal properties are modeled with the

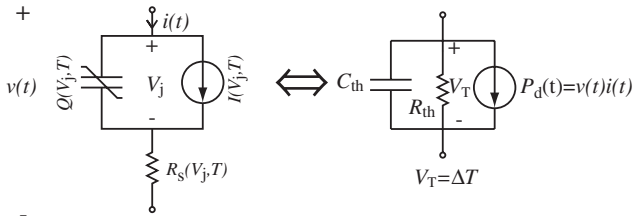


Fig. 1. (Left) electrical equivalent and (right) electro-thermal equivalent circuit model for harmonic balance simulations.

electro-thermal equivalent circuit displayed in Figure 1 (right). We have implemented the electro-thermal model in Advanced Design System (ADS) from Agilent, by using an extra nonlinear port.

III. RESULTS

A. Model verification

In order to verify the electro-thermal model, we use a well-characterized GaAs-based HBV, UVA-NRL-1174, thoroughly described in [7]. For this device, the series resistance can be approximated by

$$R_s(T) = \frac{200}{A} + \left(4 + \frac{20}{\sqrt{A}} + \frac{320}{A} \right) \frac{T}{T_0} [\Omega] \quad (10)$$

where the diode area A is expressed in μm^2 and T_0 is the ambient temperature. The thermal resistance is approximated as

$$R_{\text{th}} = \frac{15}{\sqrt{A}} [\text{K}/\text{mW}], \quad (11)$$

where, again, A is expressed in μm^2 . The conduction current is modelled with (4) with $a_{\text{GaAs}} = 170 \text{ A}/(\text{m}^2\text{K}^2)$, $E_0 = 4.2 \cdot 10^6 \text{ V}/\text{m}$ and $\phi_b = 0.17 \text{ eV}$. The thermal capacitance C_{th} is chosen so that $\tau_{\text{th}} \gg 1/f_p$ where f_p is the pump frequency. Figure 2 shows results from harmonic balance simulations with the electro-thermal model. It is clear that the measured results are modelled accurately, including the increased conduction current for high power levels, which decreases the conversion efficiency. The maximum simulated device temperature is 480 K.

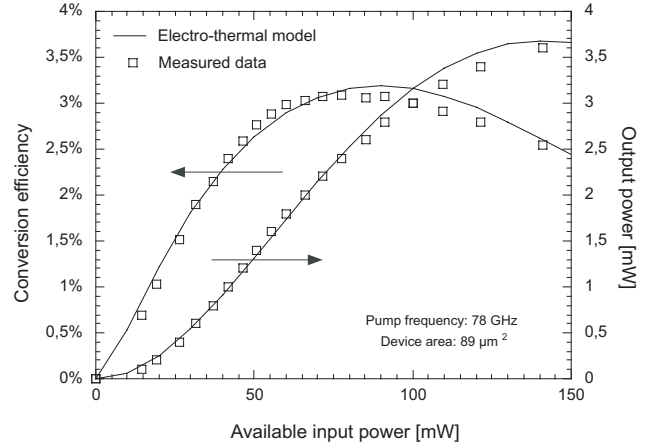


Fig. 2. Simulated and measured conversion efficiency and output power for an output frequency of 234 GHz obtained for a UVA-NRL-1174-17 HBV. For the simulations, losses of 1 dB and 2 dB are assumed at the input and output, respectively.

B. Design example

To further demonstrate the use of the electro-thermal model, we now use the model to analyze the expected performance of a 141-GHz HBV tripler source. We assume the high-power multi-mesa HBV geometry presented in [6] and a two-barrier InGaAs/InAlAs on InP layer structure with $N_d = 10^{17} \text{ cm}^{-3}$. This material structure

has demonstrated state-of-the-art performance for a 100-GHz HBV quintupler [14]. We assume a total cross-sectional device area of $A = 185 \mu\text{m}^2$, zero conduction current, and a thermal resistance estimated from FEM simulations to $R_{\text{th}} = 450 \text{ K/W}$. Again, C_{th} is chosen so that $\tau_{\text{th}} \gg 1/f_p$. This device geometry consists of four series-connected mesas, resulting in an 8-barrier device. The series resistance is calculated with (6), assuming $R_c \cdot A = 100 \Omega \mu\text{m}^2$ per mesa, and the room temperature value is 8Ω . The conversion efficiency excluding circuit losses together with the junction temperature is displayed in Figure 3. Approximately 500 mW of input power can

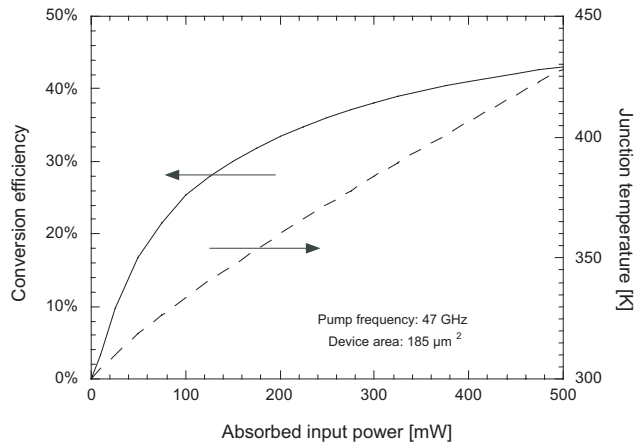


Fig. 3. Simulated diode efficiency and the corresponding junction temperature for an 8-barrier high-power HBV with an area of $A = 185 \mu\text{m}^2$.

be handled by this device without reaching the breakdown voltage per barrier or unrealistic device temperatures [9]. The maximum increase in the series resistance due to self-heating is approximately 9%. The optimum embedding impedances at the pump frequency and at the third harmonic are $Z_{1,\text{opt}} = 20 + j159 \Omega$ and $Z_{3,\text{opt}} = 42 + j69 \Omega$, respectively. Assuming circuit losses of 1 dB at the input and at the output, the flange-to-flange efficiency is about 25-30%, and the output power is approximately 170 mW for an input power of 630 mW.

IV. CONCLUSION

We have developed an electro-thermal HBV model that updates the device temperature and temperature-dependent electrical parameters self-consistently, and is thus suitable for output power optimizations. The model is especially useful for applications where the absorbed power and the conversion efficiency is unknown or difficult to estimate. It can also be used to analyze frequency multipliers with pulsed excitations of the same timescale as the thermal time constant of the device. The model presented is verified against measured results and the agreement is excellent.

ACKNOWLEDGMENT

The authors would like to thank C. Fager and E. Kollberg for help and advice. This work is supported by the European Space Agency, the Swedish Foundation for Strategic Research (HSEP), the Swedish Defence Research Agency, and the EU through the INTERACTION programme.

REFERENCES

- [1] P. H. Siegel, "Terahertz technology in biology and medicine," *IEEE Trans. Microwave Theory Tech.*, vol. 52, no. 10, pp. 2438–2447, 2004.
- [2] E. L. Kollberg and A. Rydberg, "Quantum-barrier-varactor diodes for high-efficiency millimetre-wave multipliers," *Electron. Lett.*, vol. 25, no. 25, pp. 1696–1698, 1989.
- [3] H. X. L. Liu, L. B. Sjogren, C. W. Domier, J. N. C. Luhmann, D. L. Sivco, and A. Y. Cho, "Monolithic quasi-optical frequency tripler array with 5-W output power at 99 GHz," *IEEE Electron Device Lett.*, vol. 14, no. 7, pp. 329–331, 1993.
- [4] R. Meola, J. Freyer, and M. Claassen, "Improved frequency tripler with integrated single-barrier varactor," *Electron. Lett.*, vol. 36, no. 99, pp. 803–804, 2000.
- [5] X. Mélique, A. Maestrini, E. Lheurette, P. Mounaix, M. Favreau, O. Vanbésien, J. M. Goutoule, G. Beaudin, T. Nāhri, and D. Lippens, "12% efficiency and 9.5 dBm output power from InP-based heterostructure barrier varactor triplers at 250 GHz," in *IEEE MTT-S Int. Symp. Dig.*, 1999.
- [6] A. Emadi, J. Vukusic, M. Ingvarson, T. Bryllert, Ø. Olsen, E. Kollberg, and J. Stake, "High power HBV multipliers for F- and G- band applications," in *Proc. Joint 29th IRMMW2004 / 12th THz2004*, 2004, pp. 319–320.
- [7] J. Stake, L. Dillner, S. H. Jones, C. M. Mann, J. Thornton, J. R. Jones, W. L. Bishop, and E. L. Kollberg, "Effects of self-heating on planar heterostructure barrier varactor diodes," *IEEE Trans. Electron Devices*, vol. 45, no. 11, pp. 2298–2303, 1998.
- [8] J. Stake, C. Mann, L. Dillner, M. Ingvarson, S. H. Jones, S. Hollung, H. Mohamed, B. Alderman, M. Chamberlain, and E. Kollberg, "Improved diode geometry for planar heterostructure barrier varactors," in *Proc. 10th Int. Symp. Space Terahertz Tech.*, Charlottesville, 1999, pp. 485–491.
- [9] M. Ingvarson, B. Alderman, A. Ø. Olsen, J. Vukusic, and J. Stake, "Thermal constraints for heterostructure barrier varactors," *IEEE Electron Device Lett.*, vol. 25, no. 11, pp. 713–715, 2004.
- [10] L. Dillner, J. Stake, and E. L. Kollberg, "Modeling of the heterostructure barrier varactor diode," in *Int. Semicond. Device Research Symp.*, 1997, pp. 179–182.
- [11] L. Dillner, W. Strupinski, S. Hollung, C. Mann, J. Stake, M. Beard-sley, and E. Kollberg, "Frequency multiplier measurements on heterostructure barrier varactors on a copper substrate," *IEEE Electron Device Lett.*, vol. 21, no. 5, pp. 206–208, 2000.
- [12] M. Sotoodeh, A. H. Khalid, and A. A. Rezazadeh, "Empirical low-field mobility model for III-V compounds applicable in device simulation codes," *J. Appl. Phys.*, vol. 87, no. 6, pp. 2890–2900, 2000.
- [13] S. A. Maas, *Nonlinear Microwave and RF Circuits*, 2nd ed. Artech House, 2003.
- [14] T. Bryllert, A. Ø. Olsen, J. Vukusic, T. A. Emadi, M. Ingvarson, J. Stake, and D. Lippens, "11% efficiency 100 GHz InP-based heterostructure barrier varactor quintupler," *Electron. Lett.*, vol. 41, no. 3, pp. 30–31, 2005.